LEVEL

ADA087234

High-Temperature, High-Resolution Measurements of CO_2 in the Region of 2200 to 2400 cm^{-1}.

HAJIME SAKAI
MARK ESPLIN
WILLIAM DALTON
GEORGE A. VANASSE

DTIC
SELECTED
JUL 2 8 1980
C

27 Feb 80   21

OPTICAL PHYSICS DIVISION   PROJECT 2310   G-1

AIR FORCE GEOPHYSICS LABORATORY

HANSCOM AFB, MASSACHUSETTS 01731

AIR FORCE SYSTEMS COMMAND, USAF
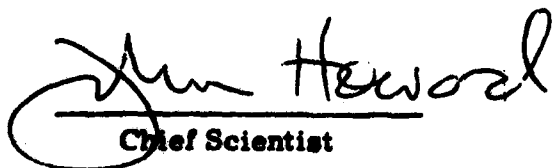
409578
80 7 28 005

This report has been reviewed by the ESD Information Office (OI) and is releasable to the National Technical Information Service (NTIS).

This technical report has been reviewed and is approved for publication.

FOR THE COMMANDER

Chief Scientist

SECURITY CLASSIFICATION OF THIS PAGE *(When Data Entered)*

REPORT DOCUMENTATION PAGE	READ INSTRUCTIONS BEFORE COMPLETING FORM

1. REPORT NUMBER	2 GOVT ACCESSION NO.	3. RECIPIENT'S CATALOG NUMBER
AFGL-TR-80-0068	AD-A087234	

4. TITLE *(and Subtitle)*	5. TYPE OF REPORT & PERIOD COVERED
HIGH-TEMPERATURE, HIGH-RESOLUTION MEASUREMENTS OF CO_2 IN THE REGION OF 2200 TO 2400 CM^{-1}	Scientific. Interim.
	6. PERFORMING ORG. REPORT NUMBER ERP No. 698

7. AUTHOR(s)	8. CONTRACT OR GRANT NUMBER(s)
Hajime Sakai[*] George A. Vanasse Mark Esplin[*] William Dalton[*]	

9. PERFORMING ORGANIZATION NAME AND ADDRESS	10. PROGRAM ELEMENT, PROJECT, TASK AREA & WORK UNIT NUMBERS
Air Force Geophysics Laboratory (OP) Hanscom AFB Massachusetts 01731	61102F 2310G101

11. CONTROLLING OFFICE NAME AND ADDRESS	12. REPORT DATE
Air Force Geophysics Laboratory (OP)	27 February 1980
Hanscom AFB	13. NUMBER OF PAGES
Massachusetts 01731	20

14. MONITORING AGENCY NAME & ADDRESS(*if different from Controlling Office*)	15. SECURITY CLASS. *(of this report)*
	Unclassified
	15a. DECLASSIFICATION DOWNGRADING SCHEDULE

16. DISTRIBUTION STATEMENT *(of this Report)*

Approved for public release; distribution unlimited.

17. DISTRIBUTION STATEMENT *(of the abstract entered in Block 20, if different from Report)*

18. SUPPLEMENTARY NOTES

Astronomy Research Facility, Department of Physics and Astronomy, University of Massachusetts, Amherst, Massachusetts

19. KEY WORDS *(Continue on reverse side if necessary and identify by block number)*

CO_2
Fourier spectroscopy

MICROMETERS

20. ABSTRACT *(Continue on reverse side if necessary and identify by block number)*

The CO_2 vibrational-rotational transition in the 4.3-μm region (2200 to 2400 cm^{-1}) was observed at an elevated temperature of 600°K. The technique of Fourier spectroscopy was used to observe the spectrum with a resolution of 0.006 cm^{-1}. The identified lines are expressed in terms of the molecular constants determined through the least-square-error fitting method. The analysis covers those bands starting from (00011-00001) through (04411-04401) for $^{12}C^{16}O_2$, through (10011-10001) for $^{13}C^{16}O_2$, (00011-00001) and

DD FORM 1473

SECURITY CLASSIFICATION OF THIS PAGE *(When Data Entered)*

20. (Cont)

(01111-01101) for $^{12}C^{16}O^{18}O$, and (00011-00001) for $^{12}C^{16}O^{17}O$.[*] The experimental instrumentation is described, with emphasis placed on the specially-constructed, high-temperature cell that is presently coupled to the Idealab interferometer located at AFGL.

---

[*] These notations for the vibrational transition are in accordance with AFGL Atmospheric Line Listing, R. McClatchey et al, AFCRL Report, AFCRL-TR-73-0096(1973).

[**] This work is supported by Air Force Office of Scientific Research.

Contents

Illustrations

Tables

High-Temperature, High-Resolution Measurements
of CO_2 in the Region of 2200 to 2400 cm^{-1}

1. INTRODUCTION

The technique of Fourier Spectroscopy was used to measure the absorption of CO_2 in the 4.3-μm region at a temperature of 600°K to a resolution better than 0.01 cm^{-1}. The Idealab 2-m path difference interferometer located at AFGL was used in conjunction with a specially-designed, high-temperature cell. The observed data were transformed into spectra and compared with simulated spectra calculated using line parameters contained in the AFGL line compilation. Discrepancies between measured and synthetic spectra were observed and new line parameters were computed from the new data for updating the AFGL line compilation. We shall describe the experimental approach and present the latest results obtained with the high-resolution, high-temperature system now in operation at AFGL.

2. DESCRIPTION OF INSTRUMENTATION

A high-temperature cell was designed and assembled by the University of Massachusetts and then coupled to the Idealab 2 m-path difference interferometer spectrometer located at AFGL. Since the 2-m interferometer spectrometer, as well as the data handling and processing of interferograms have been described

previously,[1] we shall not describe that aspect of the experiment here. However, the high-temperature cell will be described in detail because of some of its unique features and also because of its satisfactory performance.

2.1 High-Temperature Cell Design and Performance

The high-temperature cell that was designed and constructed by the University of Massachusetts is a triple-pass, 1-m long Pfund cell with f/14 optics, capable of operation up to temperatures of 1000°C. Figure 1 is a schematic of the whole hot cell assembly. The Pfund configuration was decided upon for many reasons; one main reason being that there is no necessity for elaborate alignment capabilities as required by other multi-traversal cells (like the White cell) where the number of passes can be changed by proper re-alignment of the cell mirrors. This was a critical aspect of the choice of configuration since the cell had to operate up to 1000°C and pressures from 2 to 100 Torr with a temperature gradient of less than ± 2°C over the central portion, and still maintain alignment throughout the temperature cycling. Because of the above considerations, it was decided to build a Pfund cell which would allow path lengths of 3 m to be obtained which is adequate for our measurements.
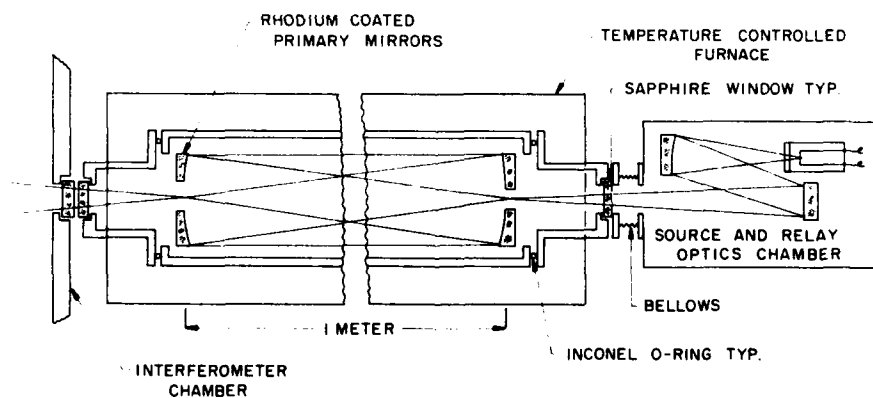

Figure 1. Schematic of Pfund Hot Cell and Source Fore-Optics Chamber

1. Sakai, H. (1977) High resolving power Fourier spectroscopy in Spectrometric Techniques I, G. Vanasse, Ed., Academic Press, N.Y.

Pritchard, J., Sakai, H., and Vanasse, G. A. (1973) AFCRL-TR-73-0233, AD 759800.

Sakai, H. (1974) AFCRL-TR-74-0571, AD A006688.

Consideration then had to be given to the type of material we would use for the tube to assure that it stood up under the harsh environment and also be easily machineable and weldable. Series 310 stainless steel has a sublimation temperature of 1385°C, well above our maximum operating temperature, with a comparatively low coefficient of thermal expansion (7.8×10^{-6} deg^{-1} and excellent atmospheric resistance to scaling. After preliminary tests on small pieces of this type of steel, it was decided to construct the entire hot-cell portion of the system out of this material. That is, the hot cell would be of stainless steel and be separate from the furnace which would surround it and heat it up to the required temperature. Even when the cell temperature reached 1000°C, it was necessary that the exterior surface of the furnace be at a relatively cool temperature for personnel safety and interferometer performance.

The furnace itself needed to be cylindrical to accommodate the gas cell and also allow easy access to the cell and the heater elements for replacement purposes. As it turned out, we were able to obtain such a furnace from the Mellen Co., Webster, N. H. who were able to take one of their stock furnaces and modify it to meet our requirements.

This furnace has been operating to our requiremence since June of 1979. We are able to keep the central 1-m section of the tube at a pre-set temperature within the ± 2°C range for periods of weeks. When turned on, the furnace reached 300°C in 2 to 3 hr and is completely stabilized after about 5 hours. The central 1-m section is monitored by thermocouples buried in the mirror end caps, and another thermocouple attached to the center of the tube. The temperature drops from 300°C at the hot cell to 50°C at the end bells of the furnace near the windows.

Having met the requirements for the hot cell and the furnace, and since we wanted to use the cell in a Pfund-type configuration, it was then necessary to decide upon the kind of substrate to use for the mirrors in the cell. Samples of fused silica, cervite, and ULE (Ultra-Low Expansion) were tested in a small furnace. The fused silica and the ULE showed no appreciable transmission or reflection losses after heating, but the cervite turned milky white and looked very much like Corning machineable ceramic. Fused silica was decided upon as substrate because of the above test and also because its coefficient of thermal expansion (0.5×10^{-6} deg^{-1}) most closely matched that of the 310 stainless steel.

Since most of the standard IR coatings such as aluminum, silver, gold, and so on, cannot be used at the temperatures mentioned above, it was decided to test the effect of temperature on the reflectivity of rhodium. After depositing a 500 Å thick film of rhodium on several pieces of polished silica, their reflectivity was measured in the 2- to 6-μm region; the results were then used for normalization. After heating them up to 300°C for a period of 24 hr, letting them cook, and measuring their reflectivity under the identical condition as prior to heating, we detected a

i

deterioration of about 10 percent in reflectivity. The same procedure was followed for temperatures of 600°C and 1000°C and the deterioration in reflectivity was found to be 30 percent and 70 percent respectively. However, the coatings did not peel but became discolored at 1000°C. Although this is not an ideal situation, the throughput of our system is adequate enough to make up for this loss (the deterioration of the mirrors with temperature would be disastrous for a multiple-traversal White cell). Two of these mirrors have been in use about 3 months at 300°C and we still observe about a 10 percent degradation in signal level; which occurred at the first use of the system.

The mirrors were mounted on a standard-type mirror holder with a ceramic fiber backing. This thin section of fiber gave the mirror just enough freedom of movement to prevent cracking. Also the ceramic fiber (made by 3M) has good chemical resistance and dimensional stability at temperatures well above 1000°C. For window material we used sapphire because of the prohibitive cost of some other materials like diamond or magnesium oxide. The sapphire transmits out to 5.8 μm and we observed no loss of transmission even when the hot cell was heated to 1000°C and cooled several times. These windows are heated to approximately 50°C and are mounted on the nose section of the hot cell (see Figure 1) on silicon O-rings to form a vacuum-tight seal.

The ends of the main tube (see Figure 1) are sealed with O-rings which separate the main tube from the short section on which the windows are mounted. This was done in order to be able to remove the short sections and have access to the cell mirrors for alignment and/or replacement purposes. The O-rings are gas-filled Inconel X750 of proper wall thickness, and allow for firm seating since Inconel is slightly softer than the 310 steel. In fact, the system can sustain a vacuum of 0.1 Torr for better than 15 hr which corresponds to a typical measurement time with the interferometer.

2.2 Light Source and Fore-Optics Assembly

The light source used consists of a specially designed chamber with a sapphire window and containing a tungsten filament heated to a temperature of 2000°C by a stabilized current and voltage output power supply. Figure 2 shows the enclosure with the tungsten filament inside it. The main body of the chamber is pyrex and because of its thermal coefficient being different from sapphire we worked our way from pyrex to sapphire by using three intermediate kinds of materials as shown in Figure 2. The tungsten source and relay optics are mounted in a separate vacuum chamber attached to the hot cell by means of a bellows; this arrangement gives access to the source and relay optics for alignment purposes without disturbing the hot cell.
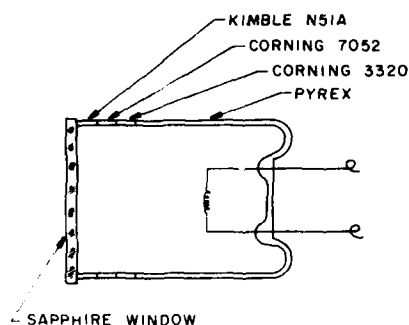
8

Figure 2. Tungsten Filament Source Enclosure

Slight realignment is required after heating; this is accomplished by peaking the detector output with a slight movement of the source relay optics. However, once the system is aligned, the hot cell can be temperature cycled many times and it will return to the same position each time. This system coupled to the high-resolution interferometer makes a very unique system for high-temperature, high-resolution studies of the absorption of atmospheric gases.

3. RESULTS

We shall now present some of the data obtained with the above instrumentation as well as the analysis which was performed by the University of Massachusetts under a grant from AFOSR. The experimental information relevant to the present data consists of:

(1) The reference frequency standard used was obtained from a single-mode frequency-stabilized He-Ne laser, the SPECTRA PHYSICS model 119. This frequency was measured to be 15798.00120 cm^{-1} by Mielenz et al.[2] All line positions were automatically calibrated against this reference laser frequency in vacuum.

(2) There is an uncertainty[3,4,5] in line position because the detector size was not accounted for; this calculated uncertainty is on the order of 0.0020 cm^{-1}. (The observed position of the $^{12}C^{16}O_2$ lines from R16 through R23 of the (0-1) band differed from those values determined by Guelachvili by 0.00206 cm^{-1} in average; which is in agreement with the calculated value of the uncertainty.)

2. Milenz, K. D., Nefflen, K. N., Gillilland, K. E., Stepens, R. B., and Zipin, R. B., (1965) Appl. Phys. Lett. 7:277.

3. Terrien, J. (1958) J. Phys. Radium 19:390.

4. Vanasse, G., and Sakai, H. (1967) Fourier spectroscopy, Progress in Optics Vol. VI, E. Wolf, Ed., North-Holland.

5. Guelachvili, G. (1973) These, Universite de Paris-Sud.

The CO_2 molecule exhibits strong absorption in the 2300 to 2400 cm^{-1} spectral region. At room temperature, the observed bands are due to transitions which involve the vibrational states of relatively low energy. As the gas temperature is elevated, the levels of higher vibrational-rotational energy are populated by means of thermal excitation and the so-called "hot" bands become observable in increased numbers. At the same time, there is a marked increase in the observable rotational lines for each vibrational band.

In the last few years there have been several studies conducted on the observable CO_2 bands in this spectral region. McCubbin et al[6] determined the molecular parameters of various transitions sequenced on the ν_3 vibrational mode by observing the emission spectra. Baldacci et al[7] subsequently conducted absorption studies in the same spectral region. Both measurements were done using conventional grating spectrometric techniques. More recently Pine and Guelachvili[8] reported the molecular parameters for the (00011-00001) band of $^{12}C^{16}O_2$ which cover from the P76 line to the R140 line. They combined two sets of data, one taken at room temperature using the technique of Fourier spectroscopy for the P and R branch lines of $J \leq 76$, and another set taken at an elevated temperature of 986°K using the technique of Frequency Difference spectroscopy for the R branch lines for $76 \leq J \leq 140$.

The present study was conducted on the absorption spectrum of CO_2 at a temperature of 600°K using the technique of Fourier spectroscopy.[9] With a spectral resolution of 0.006 cm^{-1}, our frequency accuracy was on the order of 0.002 cm^{-1}. Even though our data for the (00011-00001) band of $^{12}C^{16}O_2$ may be somewhat inferior to the data obtained by Pine and Guelachvili, the present data are a large improvement in spectral resolution and line position accuracy over data taken using grating spectrometers. The molecular parameters G, B, D and H were determined over a wide range of J values, for both the P and R branches, which become available due to the elevated temperature.

The absorptance spectrum shown in Figure 3 was obtained with a CO_2 pressure of 5.0 Torr at 600°K. It is presented to illustrate the complex structure of the spectrum and to provide an overview of the thermal excitation at this temperature. The identification of the lines was made without much difficulty for the major isotope lines which belong to the vibrational bands normally observable at room temperature. The molecular parameters given by Benedict and Rothman[10] provided an adequate base for identifying these lines even for those which originate from an extremely high J level. A degree of difficulty in identification was considerably increased for those bands which are weak at room temperature. Most of the hot bands which originate at a lower state which is higher than 2000 cm^{-1} indicated that the constants

(Due to the large number of references cited above, they will not be listed here. See References, page 20.)

given by Benedict and Rothman were rather inadequate. Their constants for the levels above 2500 cm^{-1} provided limited usefulness. Nonetheless, the identification was made for more than 1600 lines out of approximately 288 lines observed between 2200 cm^{-1} and 2400 cm^{-1} in the spectrum of Figure 3.

The result of the spectral analysis conducted on the lines identified is summarized in Table 1. The rotational constants listed in Table 1 provide the position calculated to produce the best fit for the observed lines. A range of J values in the R and P branch lines observed and the rms errors between the observed and the calculated lines for each band are listed together in the table. In determining these figures, equal weight was assigned to each position observed without discrimination for the least-square-fit computation. We thought that the weight factor which can be assigned to each line position in the data would be subject to an artificial decision, and decided that it would be replaced with a binary confidence factor indicating whether or not the observed line position in question is acceptable. Within the range shown in Table 1, very few lines were discarded from the least-square-error-fit process. The algorithm which we used to find the line center position, was not as elaborate as the one used by Guelachvili. [11] The uncertainty expected in our algorithm is about 0.001 cm^{-1}, considerably higher than the figure quoted by Guelachvili. The rms error figures were somewhat larger than 0.001 cm^{-1} probably because all observed positions were treated equally in our analysis and because the noise in the obtained spectrum was not negligible.

Four values of the rotational constants G, B, D and H of the upper state were determined for the (00011-00001), (01111-01101), (10012-10002), (10011-10001), and (00021-00011) band of $^{12}C^{16}O_2$. For the rest of the bands listed in Table 1, five constants, G, B and D of the upper state, and B and D of the lower state, were determined. These constants were determined by assuming that the vibrational-rotational level in question is given by

$$E = G + B\,J(J+1) - D\,[J(J+1)]^2 + H\,[J(J+1)]^3 .$$

Recognizing that a finite error exists in the experimental data (as indicated above) one must accept that these constants are not uniquely determined for yielding the least-square-error-fit. A strong, cross-correlation among these constants, that is, for example, a displacement in B being compensated for by a corresponding displacement in D, usually necessitates an extremely large number of independent data points to reduce their uncertainty. The spectral data inherently provide an insufficient set of data points.

11. Connes, J. (1971) Proceedings of Aspen International Conference on Fourier Spectroscopy, pp 110-112. AFCRL-71-0019, AD 722923.
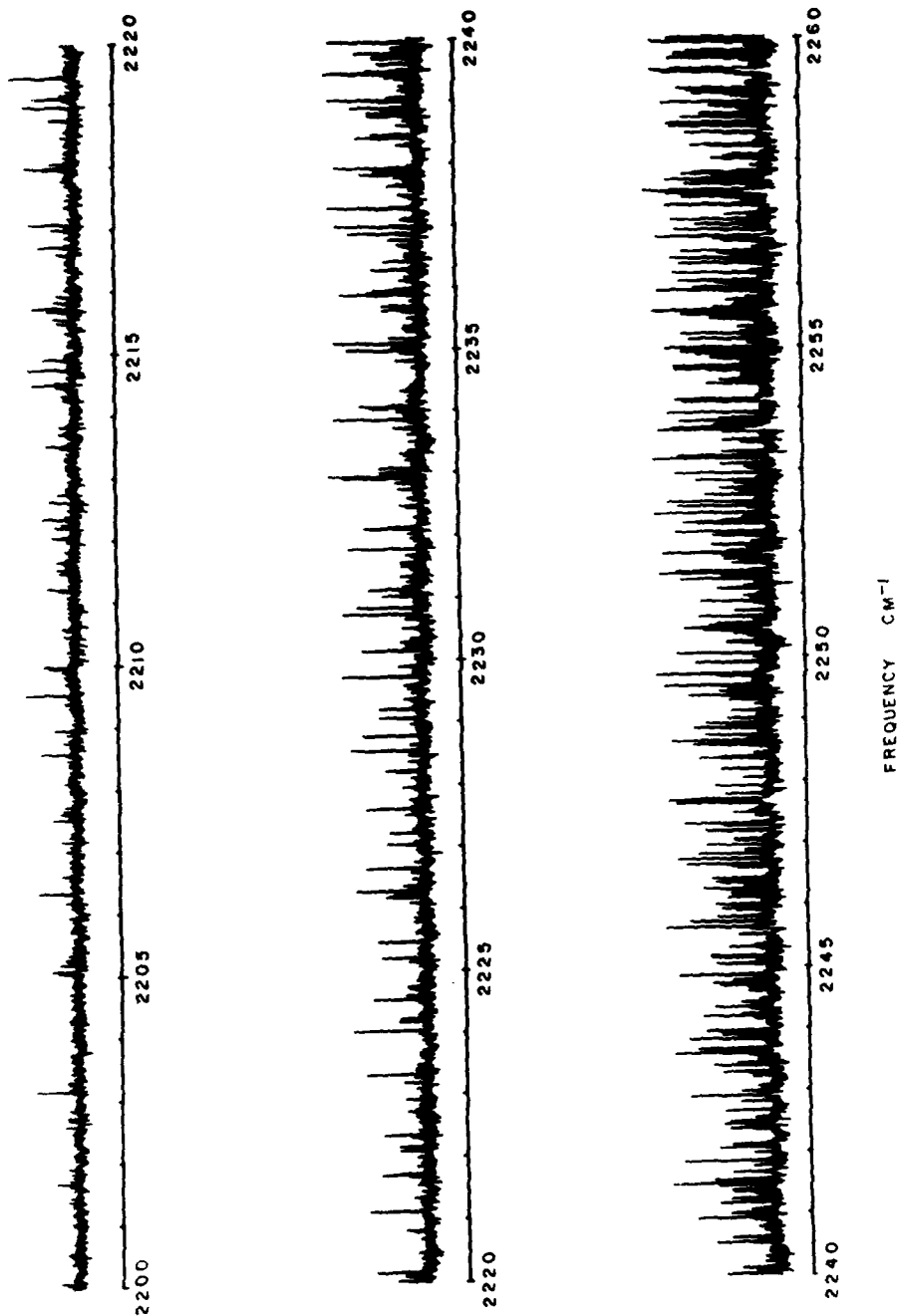
Figure 3. Spectrum of CO_2 Taken at 600° K From 2200 cm^{-1} to 2400 cm^{-1}. The plot shows the absorption vs frequency in cm^{-1}. The absorption path was 350 cm, the CO_2 pressure was 5.0 Torr and the temperature 600° K

12

FREQUENCY CM⁻¹

Figure 3. Spectrum of CO_2 Taken at 600° K From 2200 cm^{-1} to 2400 cm^{-1} (Cont)

13

Figure 3. Spectrum of CO_2 Taken at 600° K From 2200 cm^{-1} to 2400 cm^{-1} (Cont)

FREQUENCY cm^{-1}

11

FREQUENCY CM⁻¹

Figure 3. Spectrum of CO_2 Taken at 600°K From 2200 cm^{-1} to 2400 cm^{-1} (Cont)

15

Table 1. Result of Analysis Conducted on the Spectral Lines

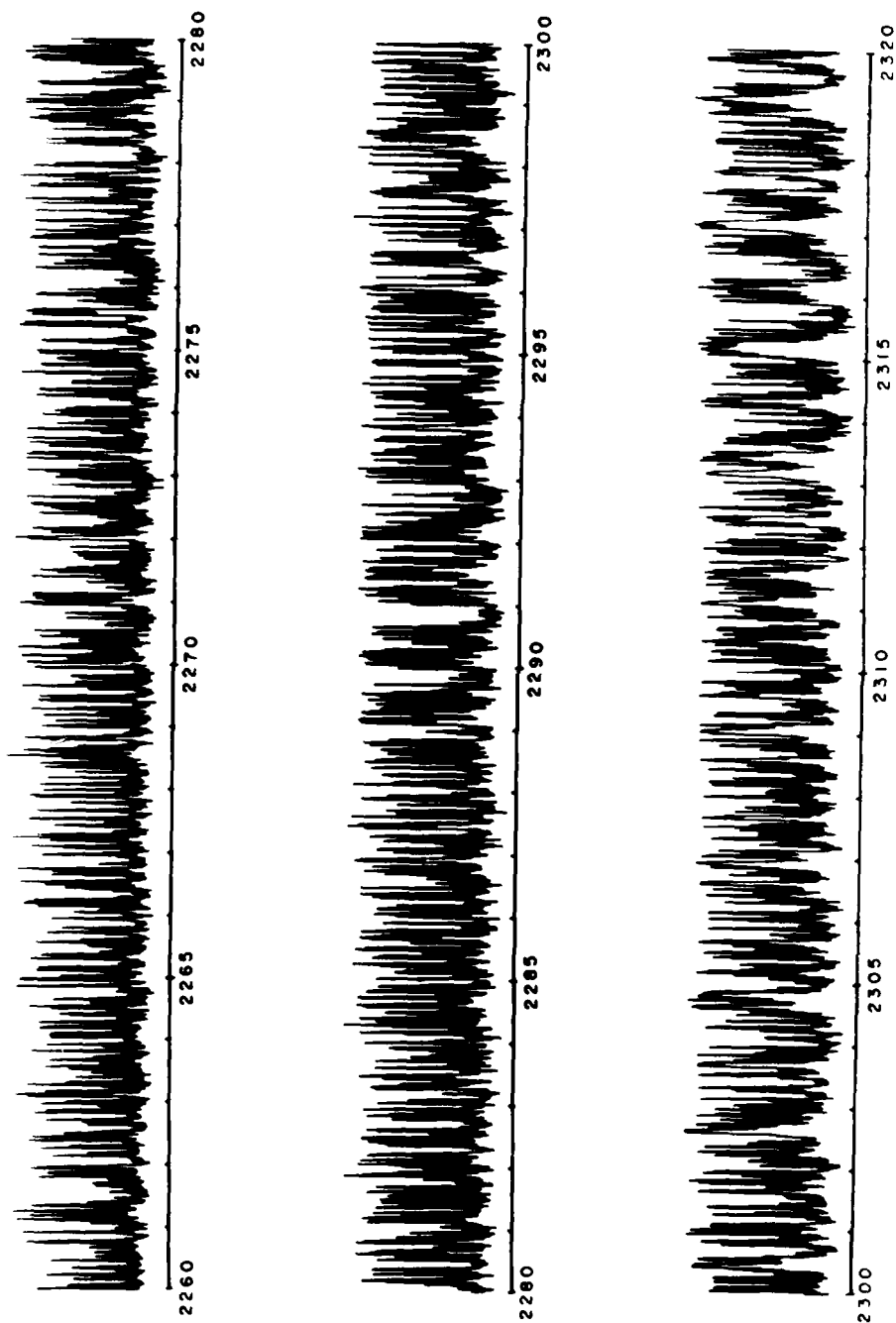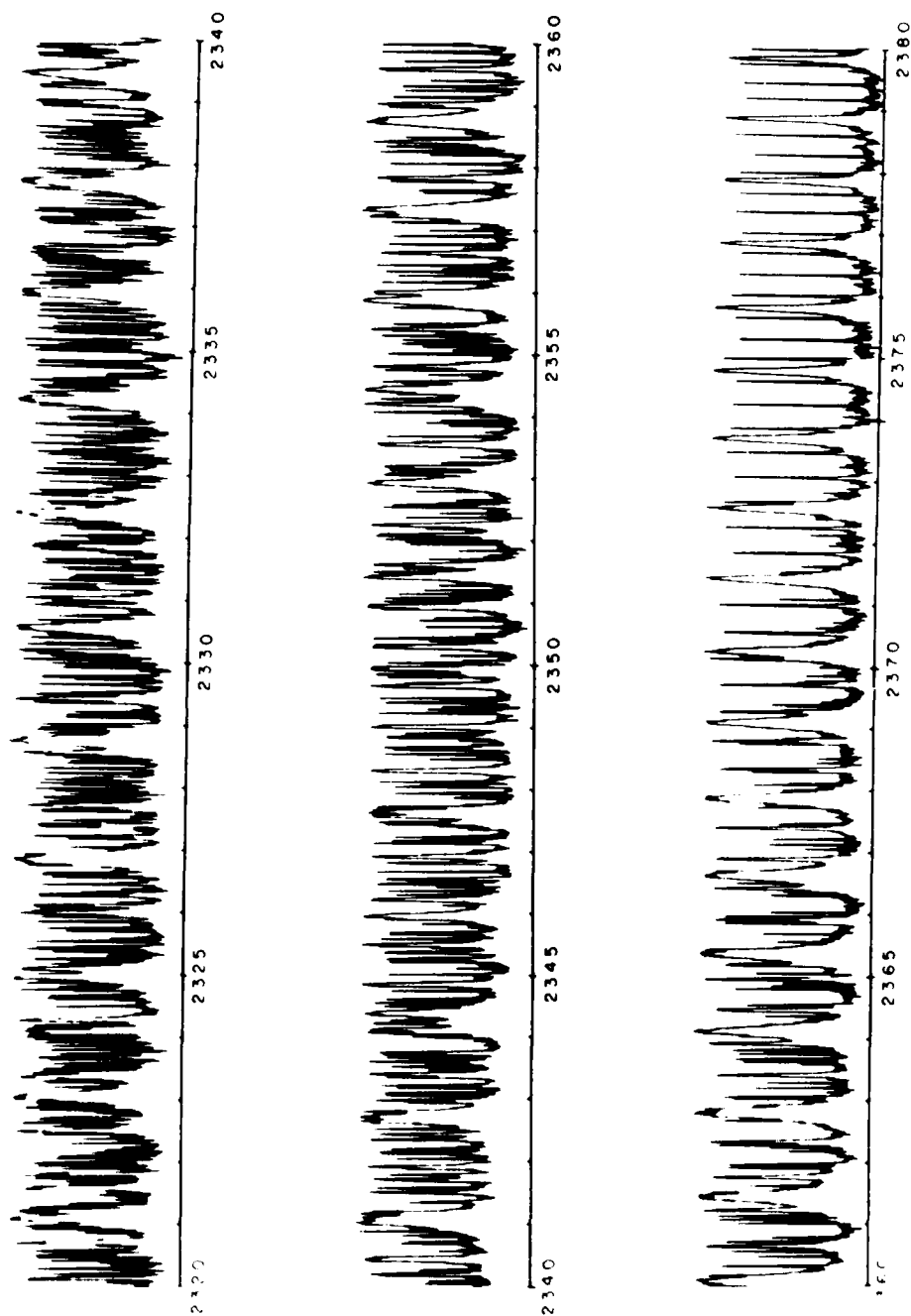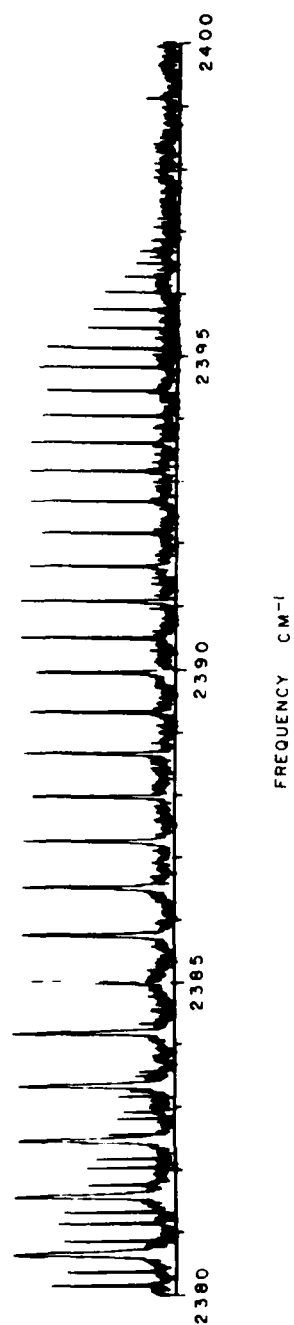| Transition	Isotope	Range of Rotational Lines Observed	G" cm^{-1}	B"	D" x10^{-7}	H" x10^{-13}	G"	B'	D' x10^{-7}	H' x10^{-13}	rms Error cm^{-1}
00011 -00001	626	P106 -R100	0.00	0.39021894	1.33373	0.1549	2349.141 (2)	0.38714209 (44)	1.33198 (54)	0.263 (59)	0.00221
00011 -00001	626	P106 -R100	0.00	0.39021960	1.33480	0.17	2349.141 (2)	0.38714273 (44)	1.33298 (59)	0.272 (59)	0.0020
01111 -01101 c	626	P99 -R89	667379	0.39064230	1.3590	0.17	3004.010 (1)	0.38759580 (35)	1.35401 (50)	0.233 (63)	0.00145
01111 -01101 d	626	P96 -R88	667.379	0.39125630	1.3610	0.17	3004.010 (1)	0.38819188 (35)	1.35785 (50)	0.190 (73)	0.00134
10012 -10002	626	P88 -R90	1285.412	0.39048227	1.57161	2.33	3612.843 (2)	0.38750266 (51)	1.57224 (84)	1.77 (12)	0.00176
02211 -02201 c	626	P86 -R82	1335.129	0.39166492 (66)	1.4095 (17)		3659.269 (2)	0.38863357 (66)	1.39331 (175)		0.00225
02211 -02201 d	626	P87 -R87	1385.129	0.39166492 (66)	1.3684 (16)		3659.269 (2)	0.38863357 (66)	1.36094 (158)		0.00225
10011 -10001	626	P86 -R86	1388.187	0.39018890	1.1495	1.19	3714.782 (3)	0.38706462 (83)	1.14549 (144)	1.32 (22)	0.00283
11112 -11102 c	626	P67 -R65	1932.470	0.39074950 (101)	1.50394 (295)		4247.704 (2)	0.38778053 (101)	1.46614 (396)		0.00217
11112 -11102 d	626	P76 -R80	1932.470	0.39168978 (59)	1.56427 (125)		4247.704 (2)	0.38870400 (59)	1.56305 (124)		0.00169
03311 -03301	626	P76 -R76	2003.238	0.39237689 (102)	1.4109 (23)		4314.904 (3)	0.38937424 (102)	1.3972 (23)		0.00275

Table 1. Result of Analysis Conducted on the Spectral Lines (Cont)

Transition	Isotope	Range of Rotational Lines Observed	G" cm⁻¹ $\mathrm{cm^{-1}}$	B"	D" $\times 10^{-7}$	H" $\times 10^{-13}$	G"	B'	D' $\times 10^{-7}$	H' $\times 10^{-13}$	rms Error $\mathrm{cm^{-1}}$
11111 -11101c	626	P71 -R71	2076.865	0.39039190 (10)	1.2386 (29)		4390.634 (3)	0.38734891 (111)	1.2257 (29)		0.00276
11111 -11101d	626	P74 -R62	2076.365	0.39133861 (128)	1.27032 (384)		4390.636 (3)	0.39823950 (130)	1.26426 (347)		0.00287
00021 -00011	626	P79 -R79	2349.141	0.38714273	1.33298	0.272	4673.323 (3)	0.38406496 (91)	1.31690 (84)	-1.4219	0.00273
20013 -20003	626	P62 -R72	2548.373	0.39111275 (12)	1.8313 (34)		4853.628 (3)	0.3882134 (12)	1.8262 (33)		0.00271
12212 -12202c	626	P54 -R52	2585.032	0.39192616 (257)	1.38506 (153)		4887.993 (3)	0.38892549 (256)	1.29089 (154)		0.00343
12212 -12202d	626	P49 -R53	2585.032	0.39192616 (257)	1.40980 (192)		4887.993 (3)	0.38892549 (256)	1.32012 (188)		0.00343
04411 -04401	626	P56	2671.690	0.39307709 (169)	1.40187 (705)		4970.901 (2)	0.39010999 (173)	1.38588 (745)		0.00221

17

Table 1. Result of Analysis Conducted on the Spectral Lines (Cont)

Transition	Isotope	Range of Rotational Lines Observed	G" cm^{-1}	B"	D" x10^{-7}	H" x10^{-13}	G"	B"	D' x10^{-7}	H' x10^{-13}	rms Error cm^{-1}
00011 -00001	636	P76 -R86	0.000	0.39023900 (158)	1.3309 (11)		2283.486 (2)	0.38727498 (58)	1.3267 (11)		0.00179
01111 -01101c	636	P65 -R63	648.484	0.39061637 (108)	1.3496 (32)		2920.242 (12)	0.38768546 (103)	1.3437 (32)		0.00216
01111 -01101d	636	P62 -R62	648.484	0.39121456 (139)	1.2846 (46)		2920.245 (3)	0.38825809 (139)	1.2645 (46)		0.00274
10012 -10002	636	P54 -R54	1265.820	0.39091320 (145)	1.5936 (66)		3527.728 (2)	0.38803309 (145)	1.5882 (66)		0.00180
02211 -02201c	636	P46 -R38	1297.269	0.39159886 (191)	1.3473 (179)		3557.316 (2)	0.38868387 (193)	1.3410 (189)		0.00196
02211 -022dd	636	P45 -R45	1297.269	0.39159886 (131)	1.3547 (159)		3557.316 (2)	0.38868387 (193)	1.3507 (159)		0.00196
10011 -10001	636	P48 R52	1370.067	0.38973653 (232)	1.2678 (115)		3632.911 (3)	0.38674792 (229)	1.28507 (112)		0.00283
00011 -00001	628	P67 -P63	0.00	0.36817722 (138)	1.1747 (39)		2332.110 (2)	0.36827919 (129)	1.1708 (40)		0.00241
00011 -00001	628	P51 -R48	0.00	0.37859562 (195)	1.2156 (100)		2340.009 (2)	0.37561681 (197)	1.2282 (102)		0.00230
01111 -01101c	628	P57 -R64	662.368	0.36861695 (220)	1.22596 (842)		2982.105 (3)	0.36574183 (220)	1.12088 (840)		0.00331
01111 -01101d	628	P58 -R58	662.368	0.36916237 (160)	1.24722 (631)		2982.103 (2)	0.36627704 (169)	1.24444 (635)		0.00271

Table 1 lists two sets of constants for the (00011-00001) band of $^{12}C^{16}O_2$, one based on the lower state constants given by Benedict and Rothman,[10] and another based on those by Pine and Guelachvili.[8] Within the range between the P106 and R100 lines, both sets produced calculated positions in good agreement with the observed positions within an rms error of 0.002 cm^{-1}. By no means do we wish to refute the constants determined by Pine and Guelachvili which yield a satisfactory fit between the P76 and R140 lines. However, we do wish to point out that the rotational constants, B, D and H, are by no means unique in yielding the best fit to the experimental data. Unique determination of these constants should be subject to other constants imposed by additional considerations from the field of molecular physics.[12] We believe that these constants can be determined by collecting more extensive data on the CO_2 vibrational-rotational transitions. In this context, the constants listed in Table 1 should be used only to calculate the line positions within the range specified.

4. CONCLUSION

The technique of Fourier spectroscopy was used to observe the CO_2 absorption at elevated temperature of 600° K. Many vibrational-rotational transitions of CO_2 thermally excited at this temperature were identified in terms of the rotational constants and the band center frequency. The data produced were indeed rich, enabling us to determine these constants using the rotational lines over a region much wider than any previously published laboratory data. Because of the extensiveness of our data, we believe that the identified lines expressed in terms of these constants will be a definite contribution in the next step for constructing the CO_2 molecular potential for the vibrational-rotational Hamiltonian which produces a global consistency over many vibrationally excited states.

12. Chihla, Z., and Chedin, A. (1971) J. Mol. Spectrosc. 40:337.

References

1. Sakai, H. (1977) High resolving power Fourier spectroscopy in Spectrometric Techniques I, G. Vanasse, Ed., Academic Press, N.Y.

   Pritchard, J., Sakai, H., and Vanasse, G.A. (1973) AFCRL-TR-73-0233, AD 759800.

   Sakai, H. (1974) AFCRL-TR-74-0571, AD A006688.

2. Milenz, K.D., Nefflen, K.N., Gillilland, K.E., Stepens, R.B., and Zipin, R.B. (1965) Appl. Phys. Lett. 7:277.

3. Terrien, J. (1958) J. Phys. Radium 19:390.

4. Vanasse, G., and Sakai, H. (1967) Fourier spectroscopy, Progress in Optics Vol. VI, E. Wolf, Ed., North-Holland.

5. Guelachvili, G. (1973) These, Universite de Paris-Sud.

6. McCubbin, T.K., Jr. Plina, J., Pulfrey, R., Telfaired, W., and Todd, T. (1974) J. Mol. Spectrosc. 49:136.

   Steiner, D.A., Todd, T.R., Clayton, C.M., McCubbin, T.K., Jr., and Polo, S.R. (1977) J. Mol. Spectrosc. 64:438.

7. Baldacci, A., Devi, V.M., Chen, D., Rao, K.N., and Fridovich, B. (1978) J. Mol. Spectrosc. 70:143.

8. Pine, A., and Guelachvili, G. J. Mol. Spectrosc., to be published.

   Guelachvili, G. J. Mol. Spectrosc., to be published.

9. Vanasse, G., Stair, A.T., Jr., and Baker, D., Eds. (1971) Proceedings of Aspen International Conference on Fourier Spectroscopy, 1970, AFCRL-71-0019, AD

10. Rothman, L.S., and Benedict, W.S. (1978) Appl. Opt. 17:2605.

11. Connes, J. (1971) Proceedings of Aspen International Conference on Fourier Spectroscopy, pp 110-112, AFCRL-71-0019, AD 722823.

12. Chihla, Z., and Chedin, A. (1971) J. Mol. Spectrosc. 40:337.